DAMPING OF SIMPLIFIED CONFIGURATIONS WITH ADDITIVES OR INTERFACES*

by

T. J. Mentel
University of Minnesota
Minneapolis, Minnesota

ABSTRACT

Recent work on simplified damping configurations is reviewed with particular emphasis on support damping mechanisms. Optimization techniques for maximizing the damping by these configurations are discussed. Some preliminary experimental results, dealing with the support damping of beams, are presented.

I. INTRODUCTION

This paper is concerned with a review of recent work on simplified damping configurations with special reference to the objective of maximizing damping. The configurations considered are divided into the four basic types shown in Figure 1. These are drawn for the case of a beam but they may also be regarded as typical plate cross sections. The first two configurations (1a and 1b), involve support interface mechanisms, while the third (1c) is a sandwich construction and the fourth (1d) is solid construction with added damping layers, or so-called damping tapes. The analysis of these four configurations is far from complete at the present time. Even the simplified methods of analysis have not been extended to all cases.

In this paper we shall be concerned primarily with only one simplified, theoretical approach which has recently been applied to these problems, and will only briefly mention a second approach. This first simplified approach sidesteps the vibration response problem by using the energy dissipation due to (inherent) material

---

*The major portion of the work reported on here was carried out at the University of Minnesota under USAF Contract No. AF 33 (616)-5426 with the Materials Central of Wright Air Development Division.

damping as a comparative reference for the energy dissipation due to the special configuration being studied, both occurring under certain assigned vibratory conditions. The success of this method depends on the relative insensitivity of these energy dissipations to the shape assumed for the vibration, so that approximate shapes fulfilling only geometric boundary conditions serve equally well as the exact shapes.

The second simplified technique, which applies only to the distributed type of damping configurations as shown in Figure 1c and 1d, involves the computation of the (complex) flexural stiffness of the composite cross-section and hence the loss factor for flexural waves. Neither the boundary conditions nor the nature of the excitation is taken into account. The damping factor is assumed small enough so that the elementary sine wave shape for the flexural waves remains valid. Also, certain neglects of the deformation of individual layers are made in order to render the analysis tractable.

In all cases, the viscoelastic material or adhesive is assumed to be describable by the hysteretic stress strain relation

$$\sigma = G_1 \gamma + G_2 \frac{1}{\omega} \frac{d\gamma}{dt}$$

for which the complex modulus is defined

$$G_r = G_1 + i\, G_2$$

The elastic and hysteretic stress coefficients, G_1 and G_2, may be given as empirical functions of temperature or frequency.

Some recent experimental work on the energy dissipation by the foregoing support damping configurations is also discussed, but since this work is still in progress, only a few preliminary results are available.

II. DAMPING DUE TO TRANSLATIONAL MOTION AT SUPPORTS

The configuration involving translational motion at supports, as shown in Figure 1a, has been redrawn in Figures 2 and 3 to define the geometry. A basic characteristic of this mechanism is that the oscillatory translational (or axial) motion

of the ends of the beam occurs at double the frequency of the originating transverse motion. The mathematical formulation of this dynamical problem, thus, is inherently non-linear in that it does not become linear as the damping is made to approach zero. This precludes an elementary solution for the vibration response characteristics. Solutions have been developed using finite degree of freedom models and iteration techniques (1), but this work is still in preparation and hence will not be discussed here.

The present review is therefore restricted to simplified analyses (2,3, and 4) which avoid involvement with the response problem. One such approach, as outlined in the Introduction, involves the computation of the energy dissipation due to both the special mechanism being studied and the material damping under certain given vibratory conditions. The subsequent order of magnitude comparison with the material damping is assumed valid if it is affected only slightly by substantial variation of the assumed vibratory conditions. Such a result has been demonstrated with respect to the shape of the fundamental mode (2) and the effect with the order of the mode will be discussed in a later section.

An additional useful simplification involves the neglect of the axial deformation of the portion of the beam in contact with the supports. The justification for this can be shown by comparing the results obtained with and without this simplification. Such a comparison is given in Figure 4 where the symbols are defined as follows:

$$h^* = h/\ell \quad , \quad m = G_1 \Big/ \sqrt{G_1^2 + G_2^2}$$

$$e = G_1/Em \quad , \quad \delta = y^{(\ell/2)}/\ell$$

The parameter $J = \ell e/c$ measures the axial stiffness of the bonded joint. In the case of a relatively stiff joint ($J = 10$), the optimum length of the bond needed to develop maximum energy dissipation is only of the order of 1 percent of the beam span, while for a highly elastic joint ($J = 0.1$) the optimum length may be of the order of the span itself. In general, as the optimum length decreases, the importance of flexibility decreases, and if the length is less than about 10 percent of the span, then the effect of end flexibility appears diminutive. Since this condition is fulfilled by most practical

designs, the neglect of end flexibility seems justified. With the foregoing simplification, the optimum value of the hysteretic stress coefficient (for the adhesive to develop maximum energy dissipation) is

$$G_2 = 1/2\ (d\ell G_1 + chE)$$

which gives the maximum energy dissipation, written in non-dimensional form, as

$$D^*_{v\,(max)} = \frac{D_v}{bh\ell E} = \frac{75.4\ h^* \delta^4}{Jmd^* + h^*} \qquad (d^* = d/\ell)$$

The material damping in a beam can be estimated using the relation

$$D_m = \int_{vol.} D\ dV$$

which, given D, yields the damping energy dissipated in inch pounds per cycle per cubic inch in a material undergoing sinusoidally varying, uniaxial stress. For our purposes, in order to provide a critical comparison with the special mechanisms, we use an empirical expression for D obtained by reading the upper limit of the scatter band of the plot of experimental values given by Lazan in reference (5). These values were obtained by testing a number of common structural materials under uniaxial stress at 20 cycles per second. The resulting expression for the energy dissipation in the material, written in non-dimensional form, is (2)

$$D^*_{m\,(max)} \equiv \frac{D_m}{bh\ell E} = 1.4 \times 10^3\ E^2 \left(\frac{\delta h^*}{S_e}\right)^3 \qquad (S_e = \text{cyclic stress sensitivity limit})$$

A comparison of the foregoing results is shown in Figure 5, where the indication is not very encouraging with respect to the translational mechanism. Only in the case of extremely thin beams, or essentially tie-rods, does this configuration offer additional damping which is greater than that already present in

the material. An indication of the way this comparison might change if higher modes were considered is given in Figure 6. The assumed modes here are those for the corresponding uniform, clamped beam without damping. Since the ratio C^2/B, which compares the two energy dissipations, other quantities being held constant, changes only by a factor of 3, the order of magnitude comparisons, which are concerned with factors of 10 or 100, would appear to be valid, at least for the lower modes of vibration.

The foregoing analysis is easily extended to the corresponding case involving circular plates (2). The optimum value of the hysteretic stress coefficient is given by

$$G_2 = ad(1 - \nu)\, G_1 + 1/2\, chE \qquad (a = \text{plate radius})$$

and the corresponding maximum energy dissipation per cycle of transverse motion (in the fundamental mode) expressed in nondimensional form, is

$$D^*_{(\max)} \equiv \frac{D}{\pi a^2 hE} = \frac{0.583}{1 - \nu} \frac{Yh^* \delta^4}{md^* + Yh^*} \qquad Y = \frac{2a(1-\nu)}{ce}$$

The estimation of the material damping, which now involves conditions of biaxial stress, appears subject to some debiety (4); nevertheless, some interesting results are indicated. In particular, a comparison for circular plates similar to that shown previously for beams is given in Figure 7. The surprising result here is that the same translational mechanism is now indicated of being capable of gross additions to the total energy dissipation for a large range of practical plate geometries. The reasons for this difference in the results between the beam and the circular plate appear to lie in the more favorable depth to span ratios and the predominancy of dilatational straining which occurs for the plate.

It is of interest to note that if dry surface (or Coulomb friction) contact is used instead of the viscoelastic adhesive, and the normal pressure is adjusted so as to maximize the energy dissipation, the maximum value of this dissipation is only 64 percent of that for the corresponding viscous case (2). This appears to be a fortunate characteristic in view of the fretting problem associated with dry friction.

The more difficult problem of the square plate has also been solved in the manner of the foregoing circular plate problem, and similar results have been obtained (3). Because of its practical importance, a plot of the variation of the dissipation with the stress coefficients for the adhesive is shown in Figure 8. The mathematical expressions are not given on account of their algebraic complexity. A design curve based on these results is shown in Figure 9. To use this curve, it is necessary only to substitute the relevant data into the expressions for p and q, leaving at least one parameter to be adjusted. The matching combinations of p and q, which maximize the energy dissipation, are then read from the curve.

III. DAMPING DUE TO COMBINED TRANSLATIONAL AND ROTATIONAL MOTION AT SUPPORTS

Recent experimental work (4) has shown that small rotational displacements within a bonded joint, as indicated in Figure 1b, can give rise to comparatively large energy dissipations. The actual deformation process within the joint, of course, is considerably complicated by the non-uniform flexural deformation of the beam and the lateral flow of the adhesive. However, if the built-in portion of the beam is assumed rigid, so that the motion is reduced to the sum of a rotation and a translation, then an elementary solution is possible. If the translation is next assumed to be zero, then the mathematical problem is linearized, and closed form solutions for the associated dynamical problem are available for both the beam and the circular plate (6).

For our present review, however, we retain the translational motion and deal with the resulting non-linear problem in a manner analogous to the previous case. The objective is to assess the relative importance of the rotational and translational motions as they occur simultaneously. Of course, certain basic differences between the damping effects of these mechanisms are readily apparent. For example, the rotational mechanism is insensitive to those flexural waves which have nodes exactly at the support boundary (as would occur for all waves for infinitely rigid supports), while the translational mechanism must sense all flexural waves irrespective of their location.

A suitable shape for the vibration for applying the aforementioned comparative type of analysis to this problem is assumed

to be given by the corresponding undamped beam with elastically hinged ends. The solution for this case, of course, is readily obtained and the frequency equation is found to contain the following parameter:

$$r = \frac{12 \ell_\theta \ell \, d^2 G_1'}{cEh^3}$$

where ℓ_θ and G_1' are defined by the immediately following equations. The axial force and end moment developed at the supports is expressed by

$$N = \frac{2bd}{c} \left(G_1 s + \frac{G_2}{} \frac{ds}{dt} \right)$$

$$M = \frac{\ell_\theta \, bd^2}{c} \left(G_1' \theta_o + \frac{G_2'}{} \frac{d\theta_o}{dt} \right)$$

The reference length is thus seen to account for the flexing of the beam and flow of the adhesive. This may be an oversimplification in that one such parameter may not be sufficient to account approximately for these effects over a useful range, but no further generalization will be considered. The primes are used to denote possible variation in the stress coefficients from those applying to the simple shear case. It is believed that the damping action results from shear deformation due to the (oscillatory) lateral flow of the adhesive, i.e., a pumping action, but this remains to be established.

The energy dissipation per cycle of transverse motion is found to be*

$$D_{V\theta}^* \equiv \frac{D_{V\theta}}{bh\ell E} = P \cdot \frac{\ell_\theta \, d^2}{ch\ell E} \, G_2' \, \delta^2$$

$$D_{Vs}^* \equiv \frac{D_{Vs}}{bh\ell E} = Q \cdot \frac{\frac{d\ell G_2}{chE} \delta^4}{\left(\frac{2d\ell G_2}{chE} \right)^2 + \left(\frac{d\ell G_1}{chE} + 1 \right)^2}$$

---

*Unpublished work of Mentel and Fu.

where a typical set of values are

r	10^{-2}	1	10^{2}
P	0.97	50.75	1.55
Q	18.4	18.2	18.1

A plot of these results for a given set of parameters is shown in Figure 10. For simplicity, only one magnitude for the resultant complex modulus is used. This is achieved by setting $|G_r| = 10^5$ so that $G_1 = |G_r| \cos\theta$ and $G_2 = G_r \sin\theta$. Allowing θ to vary from 0 to 90 degrees thus has the effect of ranging from a pure elastic to a pure viscous adhesive (keeping the resultant stiffness fixed). The graphical plot shows that the rotational damping mechanism is considerably more effective than the translational mechanism, at least for the fundamental mode. The precise meaning of this for the dynamical response problem, however, remains to be examined.

It is of considerable interest to ascertain what type of bonded joint is needed to produce an effective rotational damping mechanism. An experimental program has recently been initiated at the University of Minnesota to investigate this and other questions arising with respect to support damping mechanisms and a few preliminary results which have been obtained are reviewed next.

An overall view of the experimental apparatus is shown in Figure 11, with a close-up of a model beam under test shown in Figure 12. The initial runs were made with aluminum beams of the type shown in Figure 13. The ends, which were clamped between steel blocks, were flared so as to provide a large, stiff area for the adhesive. Small cantilever extensions at the center span provided an attachment point remote from the main flexural straining action, for the shaker unit. A typical set of results for one of the beams is shown in Figure 14. These results were obtained by vibrating the beam at system resonance. The relatively large central mass (shaker and dynamometer assembly) had the effect of making the system behave like a one degree of freedom set-up, which was precisely one of the conditions assumed in the theoretical analysis.

If the dissipation at the supports of the foregoing model beam was of the type indicated in Figure 1a, then the energy dissipation should have increased as adhesive was introduced

up to a thickness of about 0.002 inch , and then decreased for greater thicknesses. This clearly did not occur. The reason for this disparity is evident in Figure 15 which shows the shape of the fundamental mode. Pronounced rotation at the supports is readily apparent for the case of the large thickness of adhesive, and this motion can be easily shown to be able to account for the added energy loss (4). The conclusion here appears to be that an effective rotational damping mechanism can be developed by only a few thousandths of an inch thickness of viscoelastic adhesive, and thus may be one of the easiest mechanisms to construct in practice. In fact, it appears that adhesive need only be introduced along the edges of the support junction, with the resulting limited penetration being sufficient. This problem is currently under study at the University of Minnesota.

In order to separate the effects of the rotational and translational mechanisms, an articulated model, comprised of two stiff, steel sections, was constructed as shown in Figure 16. The set-up for achieving rotational motion only is shown in Figure 16a, while that for achieving translational motion only is shown in Figure 16b. A photograph of the actual set-up for the translational case appears in Figure 17. Preliminary results using this model appear to verify the theory for the translational case. The analysis for the rotational case, particularly with respect to accounting theoretically for the end moment, is not yet complete.

IV. DAMPING BY DISTRIBUTED CONFIGURATIONS

The sandwich beam with a centrally located, viscoelastic core, as shown in Figure 1c, has been analyzed by the comparison method given in the preceding cases (2), as well as by the technique of estimating the loss factor for flexural waves (7). The results of the former analysis show that if design parameters are suitably optimized, the energy dissipation per cycle of motion in the fundamental mode (for a built-in beam) can exceed the material damping by possibly two orders of magnitude. The mathematical results will not be presented on account of their algebraic complexity, but certain numerical results are shown in Figures 18, 19, and 20. Figure 18 shows a comparison of the translational, sandwich, and material damping for beams for a case where the translational mechanism is indicated to have little effect. The foregoing conclusion, with respect to sandwich

damping, appears to be substantiated by this graph. Figure 19 shows an optimization, for maximum energy dissipation, of a sandwich beam geometry for a given viscoelastic adhesive. Figure 20 shows another method of optimization, this time keeping the geometry fixed and varying the properties of the adhesive. Both of these optimizations apply only to the fundamental mode for a built-in beam and involve somewhat tedious numerical work (2).

The second approximate approach, involving the loss factor, has been carried out by Ross, Kerwin, and Dyer (7). This will be described by them in a later paper in this symposium.

The final mechanism referred to at the beginning of this paper involved the use of damping tape or some equivalent system of alternate layers of adhesive and septum. A simplified version of this mechanism was studied by Whittier (8), who investigated the occurrence of optimum configurations of a single adhesive and septum layer for a cantilever beam when vibrated at a frequency considerably below its first resonance. A more general study, based on the computation of the loss factor, has been carried out by Bolt Beranek Newman, Inc., and this work will be described in a forthcoming session.

V. CONCLUSIONS

No complete analyses are yet available for the design of dampled structures employing the simplified configurations discussed in this paper. Certain analyses, however, have been carried forward to the point where optimum design characteristics, defined under various restrictions such as the absence of higher modes, remoteness of boundaries, sinusoidal excitation, etc., can be estimated for given cases. The development of more comprehensive analyses, however, appears very promising and is proceeding from several directions. At the University of Minnesota, for example, the approximate analysis of the response problem for the non-linear support damping case has been completed and experimental work is now underway on the damping of plates.

Substantial progress has also been made with respect to the alternate viscoelastic and elastic layer configurations, and this will be reported on in a later session.

BIBLIOGRAPHY

1. Mentel, T. J., and Fu, C. C., "Response of Beams With Longitudinal and Rotational Dissipation Mechanisms at the Supports," Report of the University of Minnesota to Wright Air Development Division (Recently published as WADD Technical Report 60-60, May 1960).

2. Mentel, T. J., "Damping Energy Dissipation by Interfaces in Beam and Plate Supports and in Sandwich Cores," WADC Technical Report 58-547, December 1958.

3. Mentel, T. J., and Fu, C. C., "Damping Energy Dissipation at Support Interfaces of Square Plates," WADC Technical Report 59-96, June 1959.

4. Mentel, T. J., "Vibrational Energy Dissipation at Structural Support Junctions," paper presented at ASME Meeting, Atlantic City, December 1959.

5. Lazan, B. J., "Damping and Resonance Fatigue Behavior in Materials," Proceedings of the Int. Cong. of Fatigue of Metals, London, September 1956.

6. Das, Y. C., "Quasi-Orthogonal Modes of Dynamical Systems," Ph.D. Thesis, University of Minnesota, 1959.

7. Ross, D., Kerwin, E. M., Jr., and Dyer, I., "Flexural Vibration of Multiple-Layer Plates," Report of Bolt Beranek Newman, Inc. to ONR, June 1956.

8. Whittier, J. S., "Effect of Configurational Additions Using Viscoelastic Interfaces on the Damping of a Cantilever Beam," WADC Technical Report 58-568, May 1959.

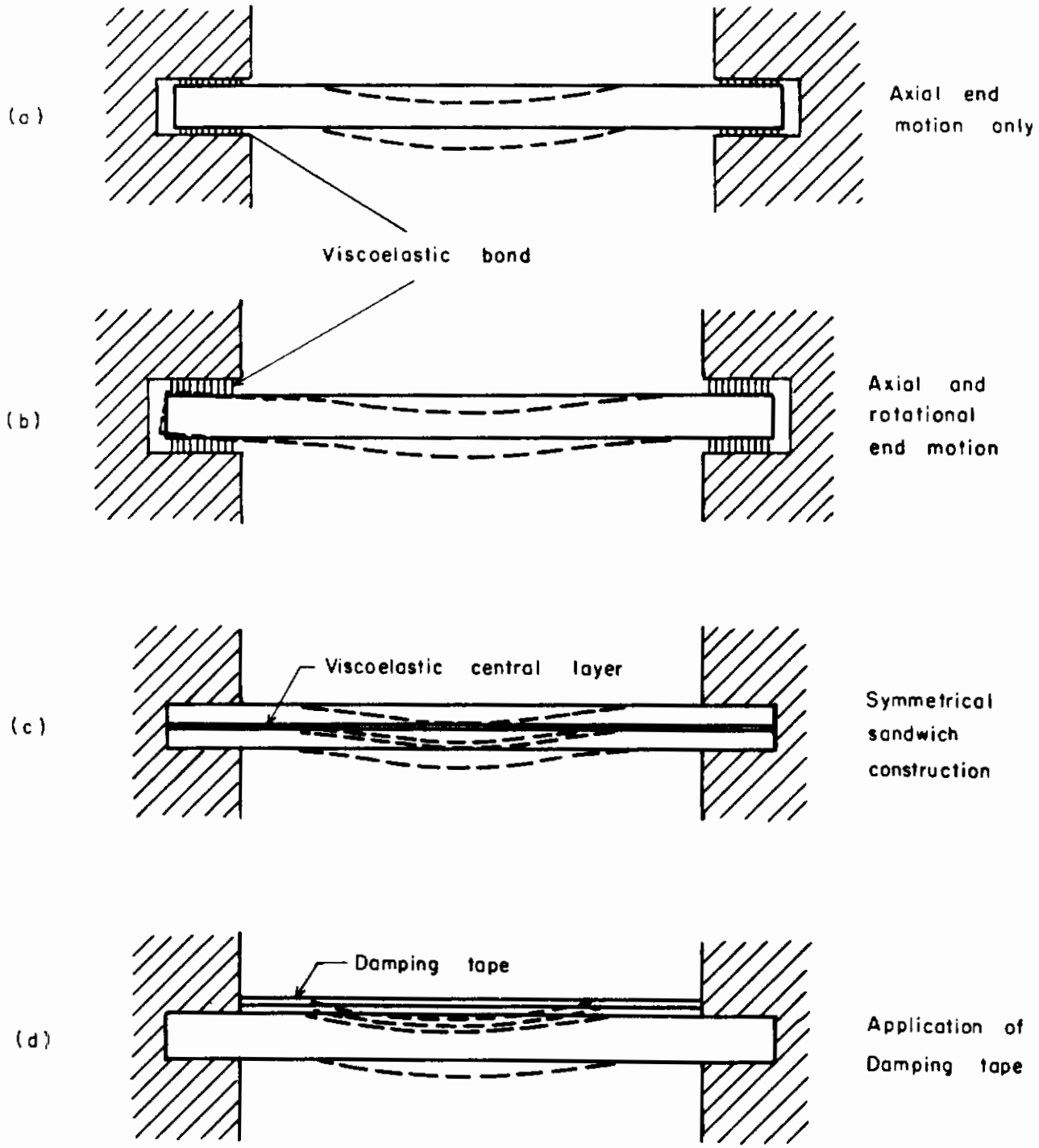

Fig. 1 Simplified Damping Configurations

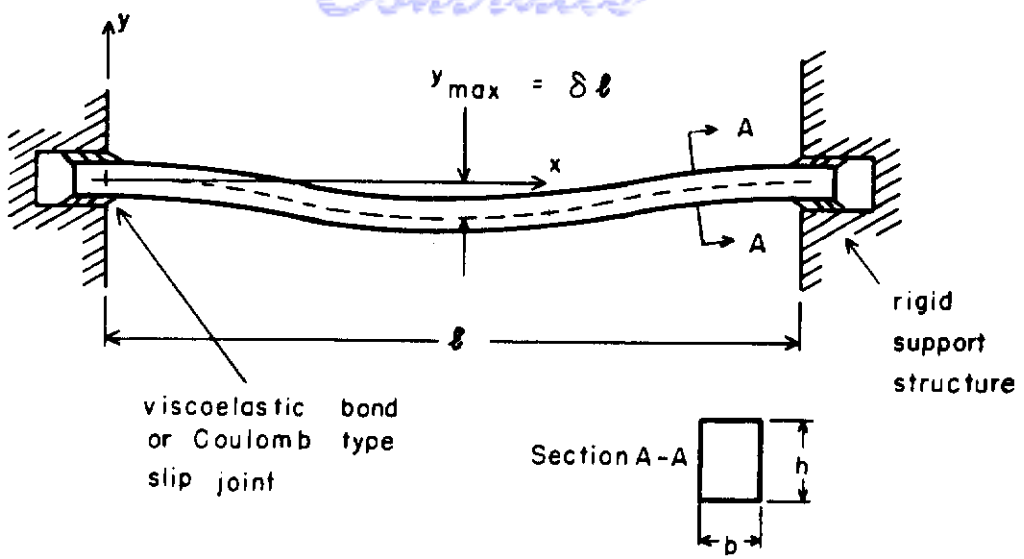

Fig. 2 Overall Beam Geometry.

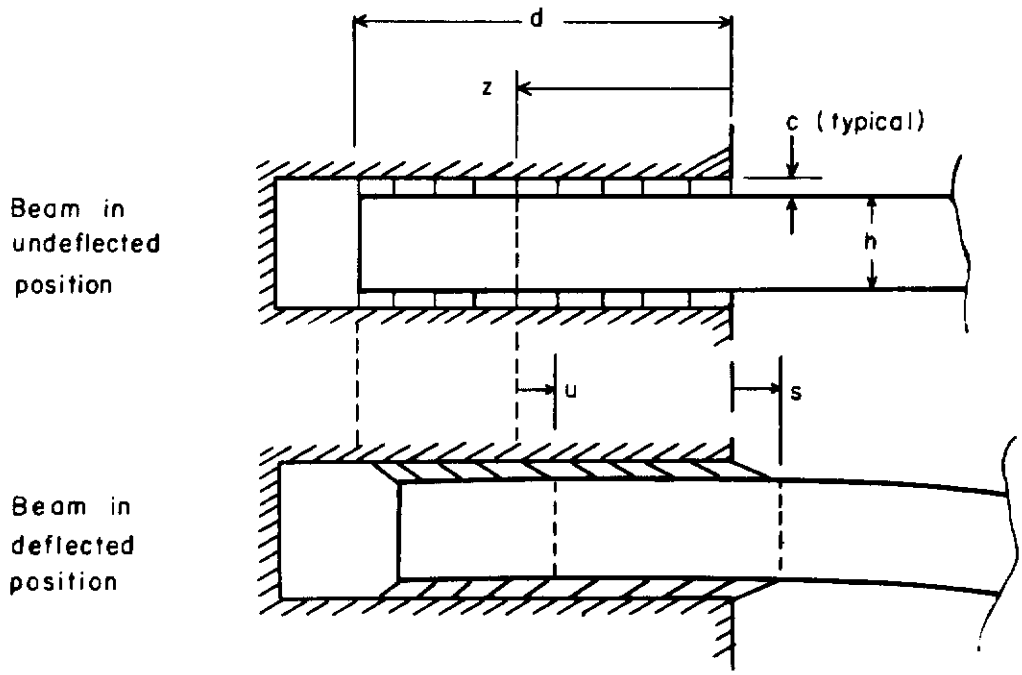

Fig. 3 Support Geometry.

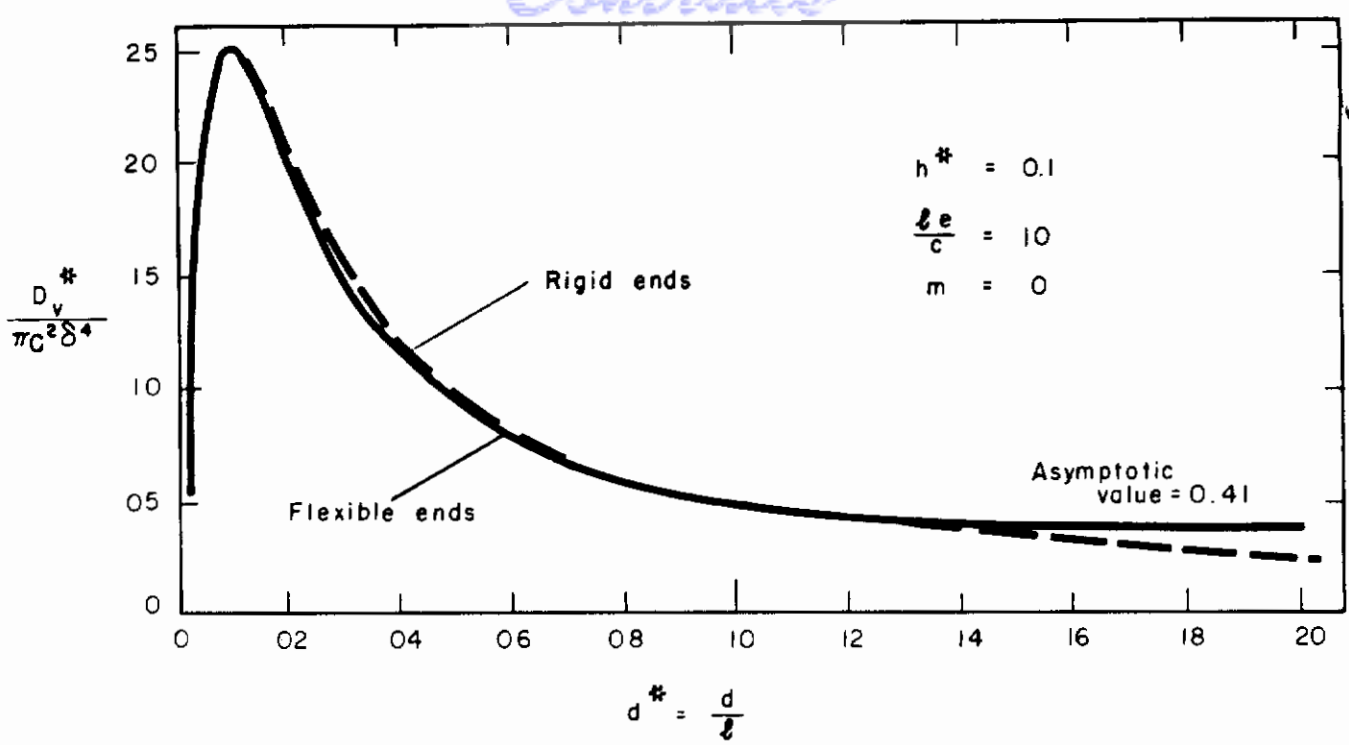

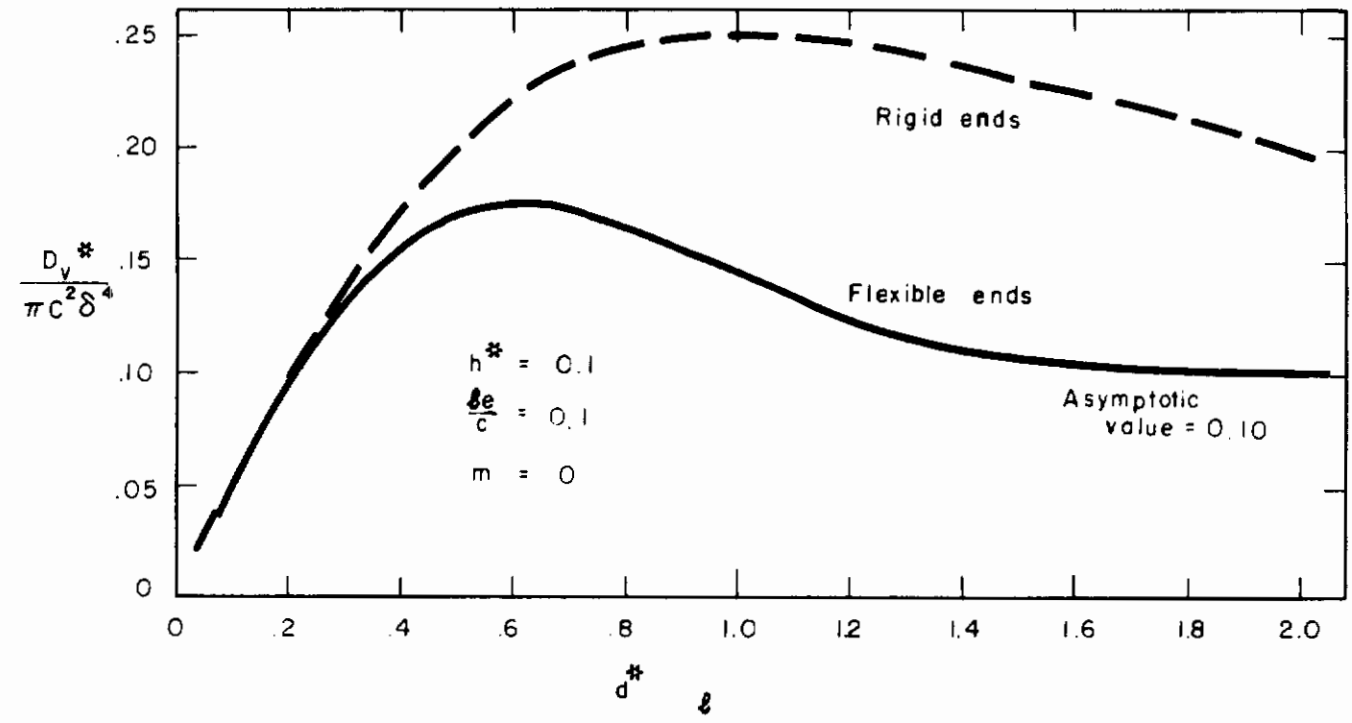

Fig. 4 Effect of End Flexibility.

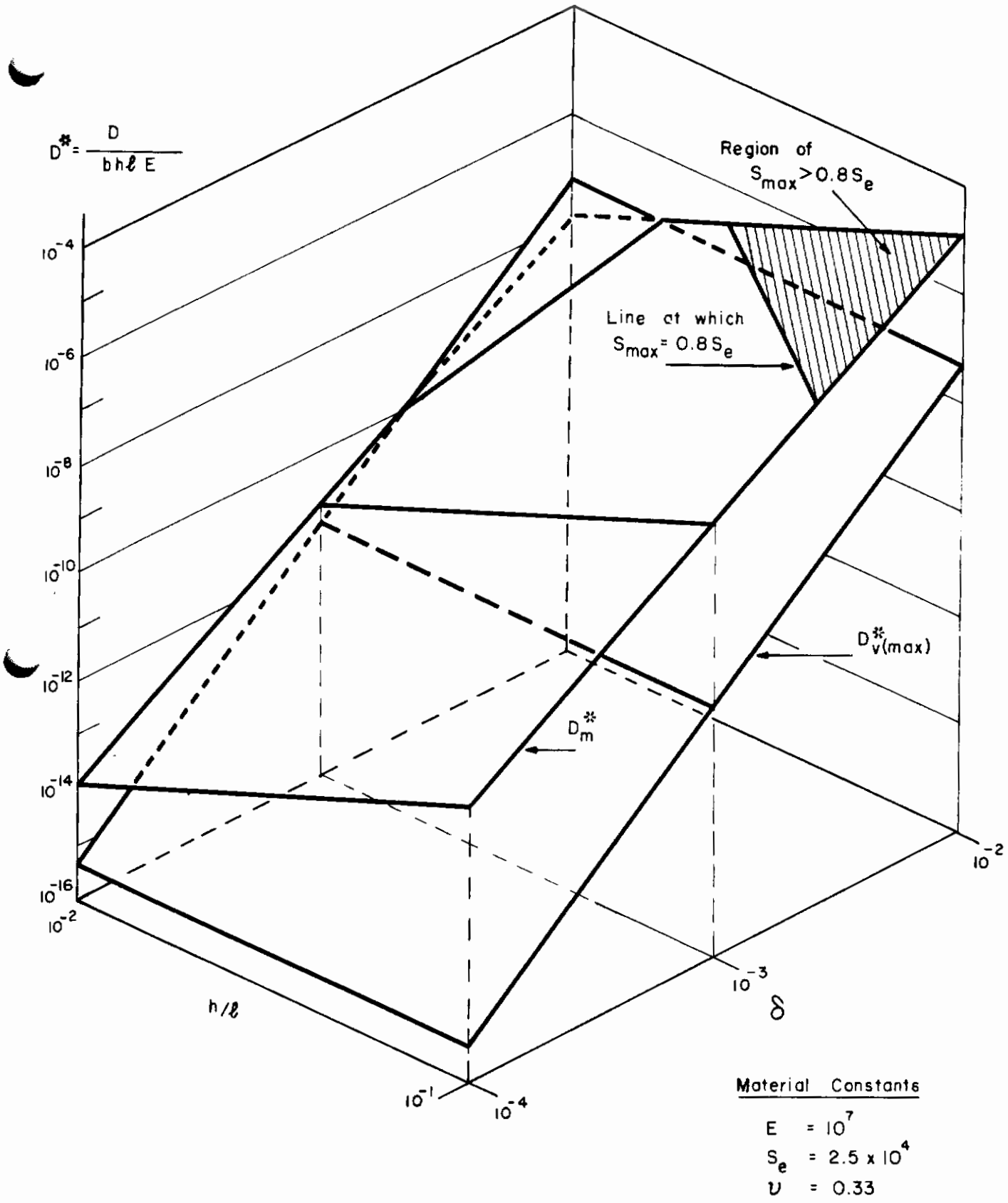

Fig. 5 Comparison of Energy Dissipation for Beams

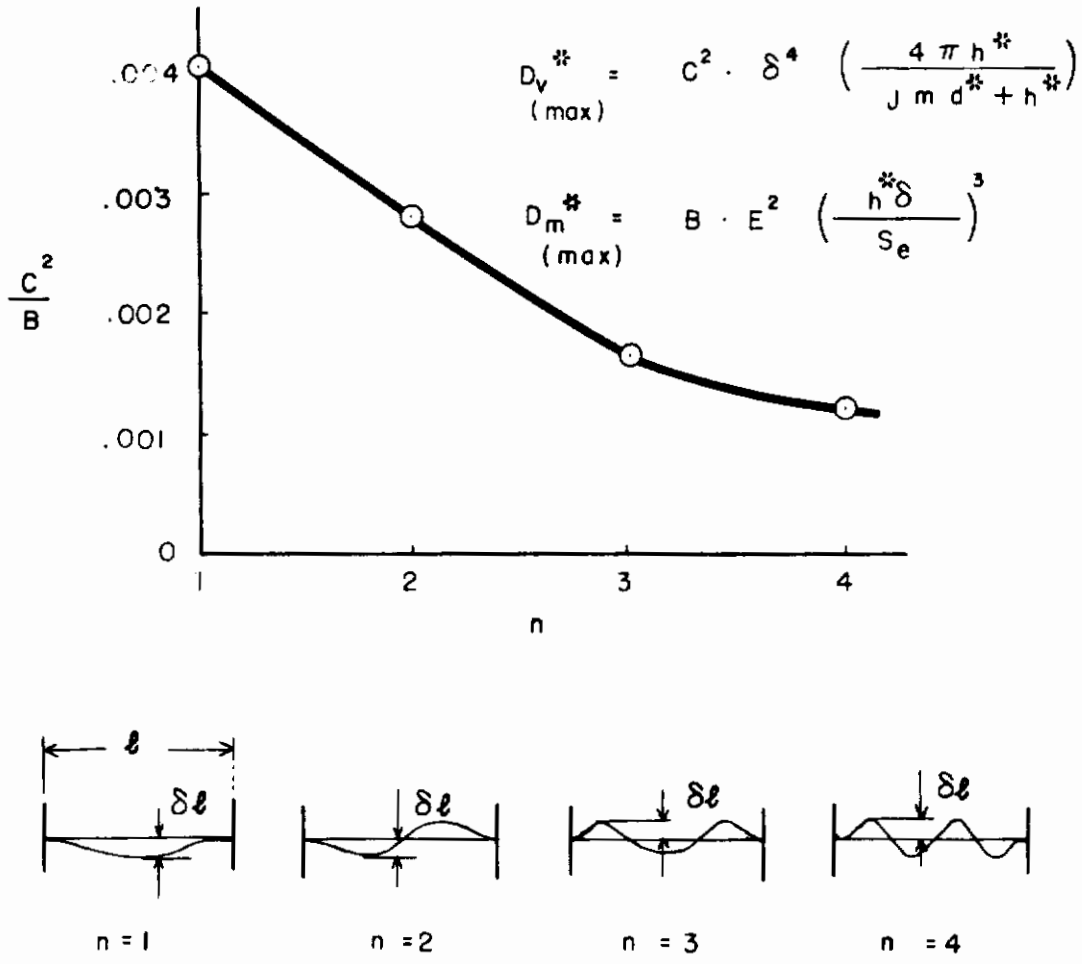

Fig. 6 Effect of Higher Modes.

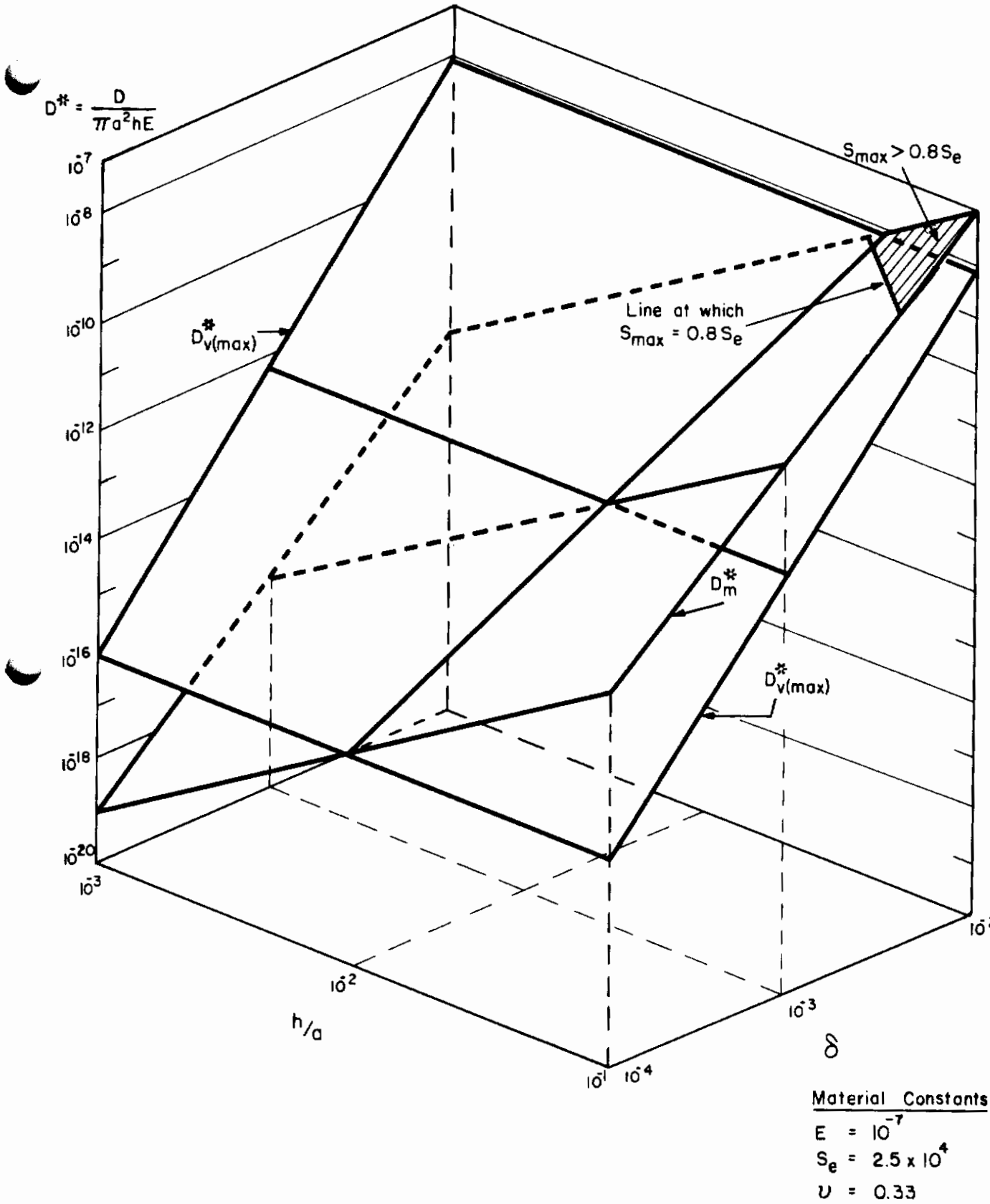

Fig. 7 Comparison of Energy Dissipation for Circular Plates.

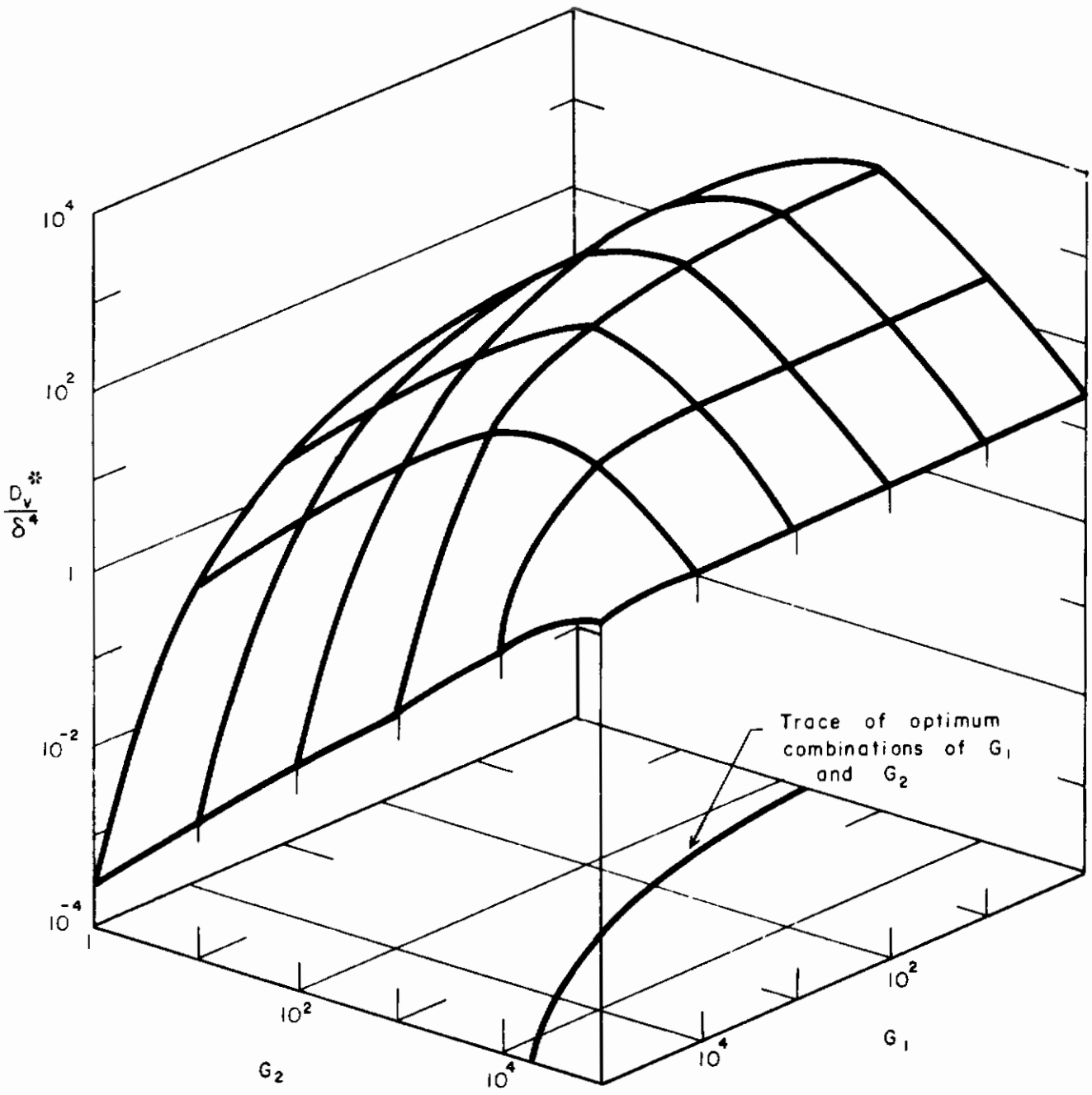

Surface plotted for $\frac{\sqrt{2}\, d\, \ell}{h c \mu} = 5 \times 10^{-3}$

$\nu = 1/3$

Fig. 8 Energy Dissipation at Support Interfeces of a Square Plate.

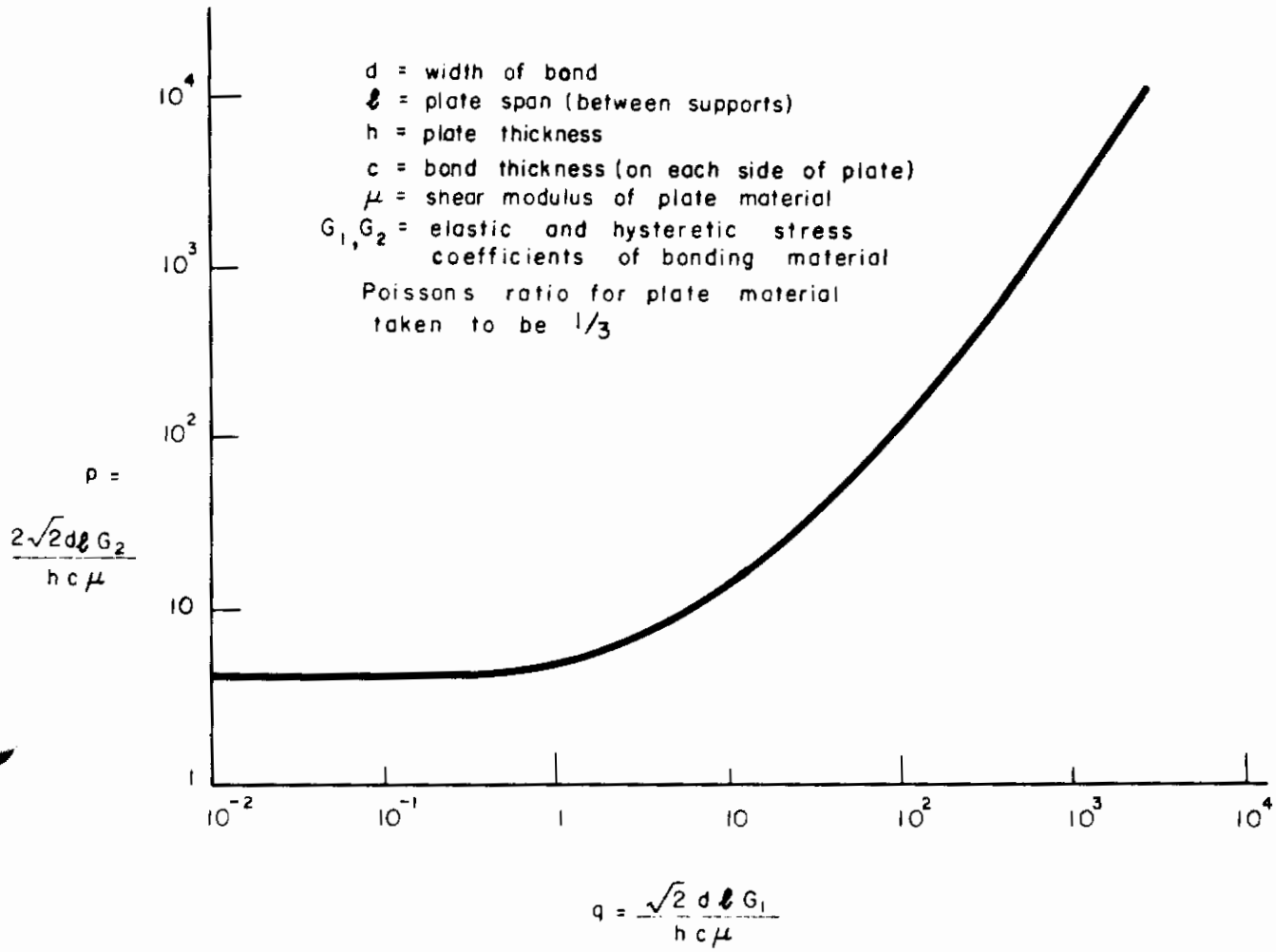

Fig. 9 Design Curve for Maximizing Energy Dissipation at Support Interfaces of a Square Plate.

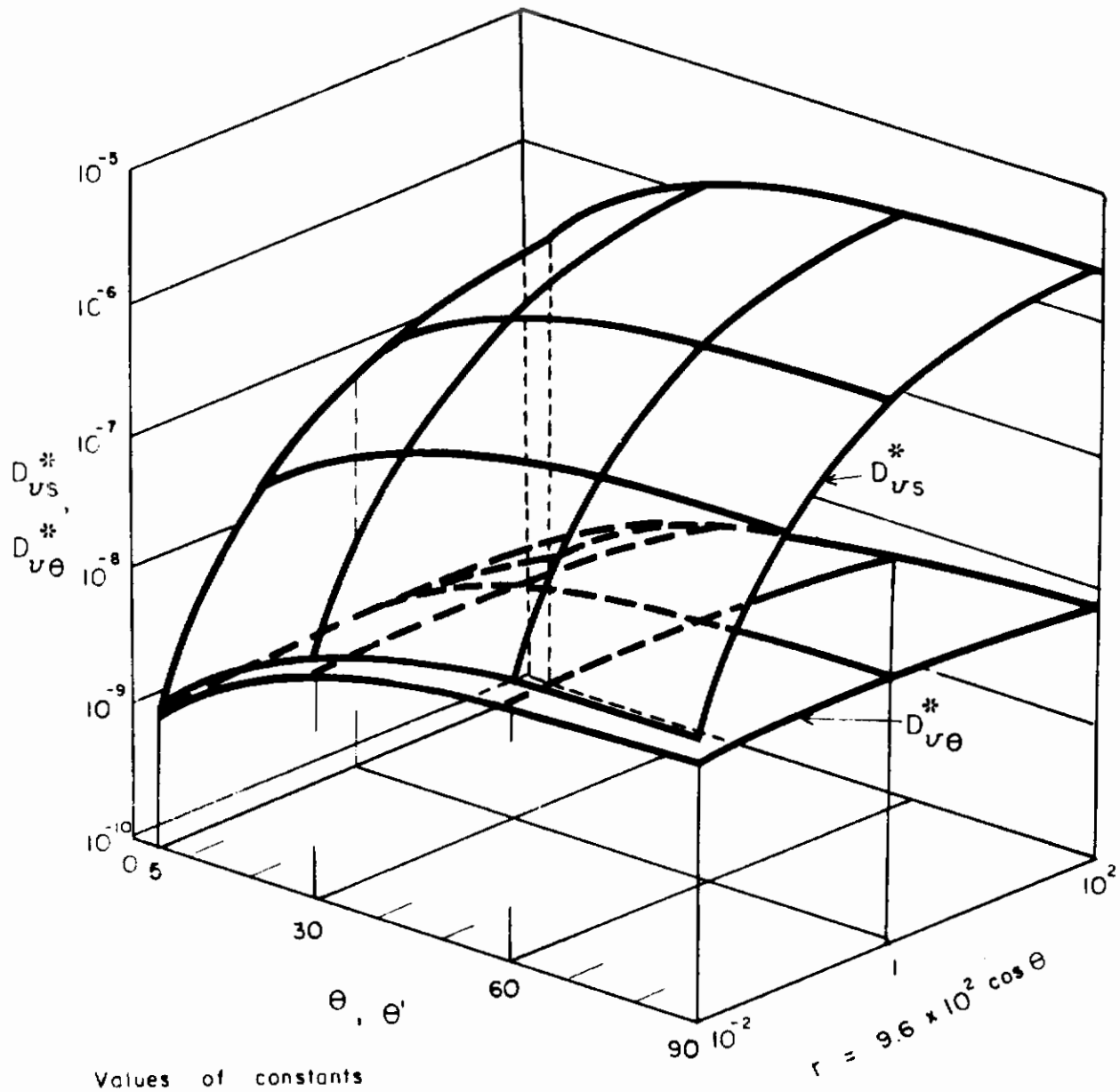

Values of constants

$\delta = 10^{-2}$ $\quad h^* = 0.05$

$d^* = 0.1$ $\quad J = 2$

$|G_r| = 10^5$ $\quad E = 10^7$

Fig. 10 Comparison of Translational and Rotational Damping.

Fig. 11 Overall View of Experimental Set-Up

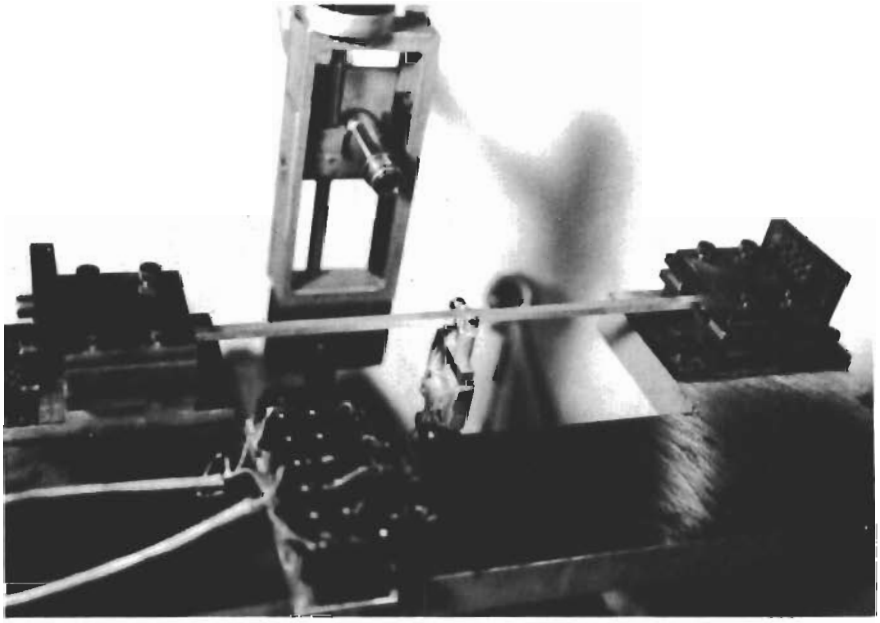

Fig. 12 Model Beam Under Test

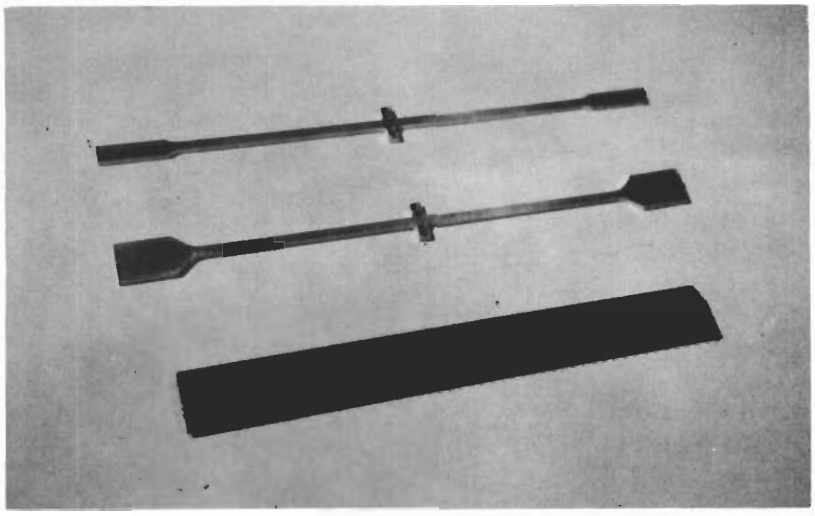

Fig. 13 Model Beam Specimens

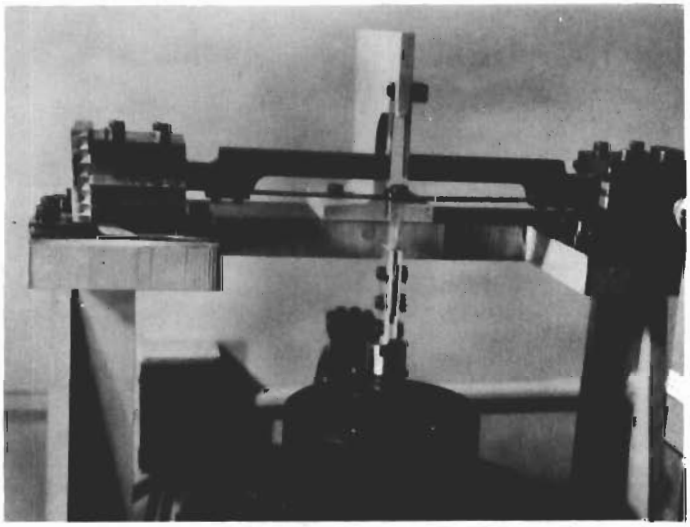

Fig. 17 Translational Configuration Set-Up

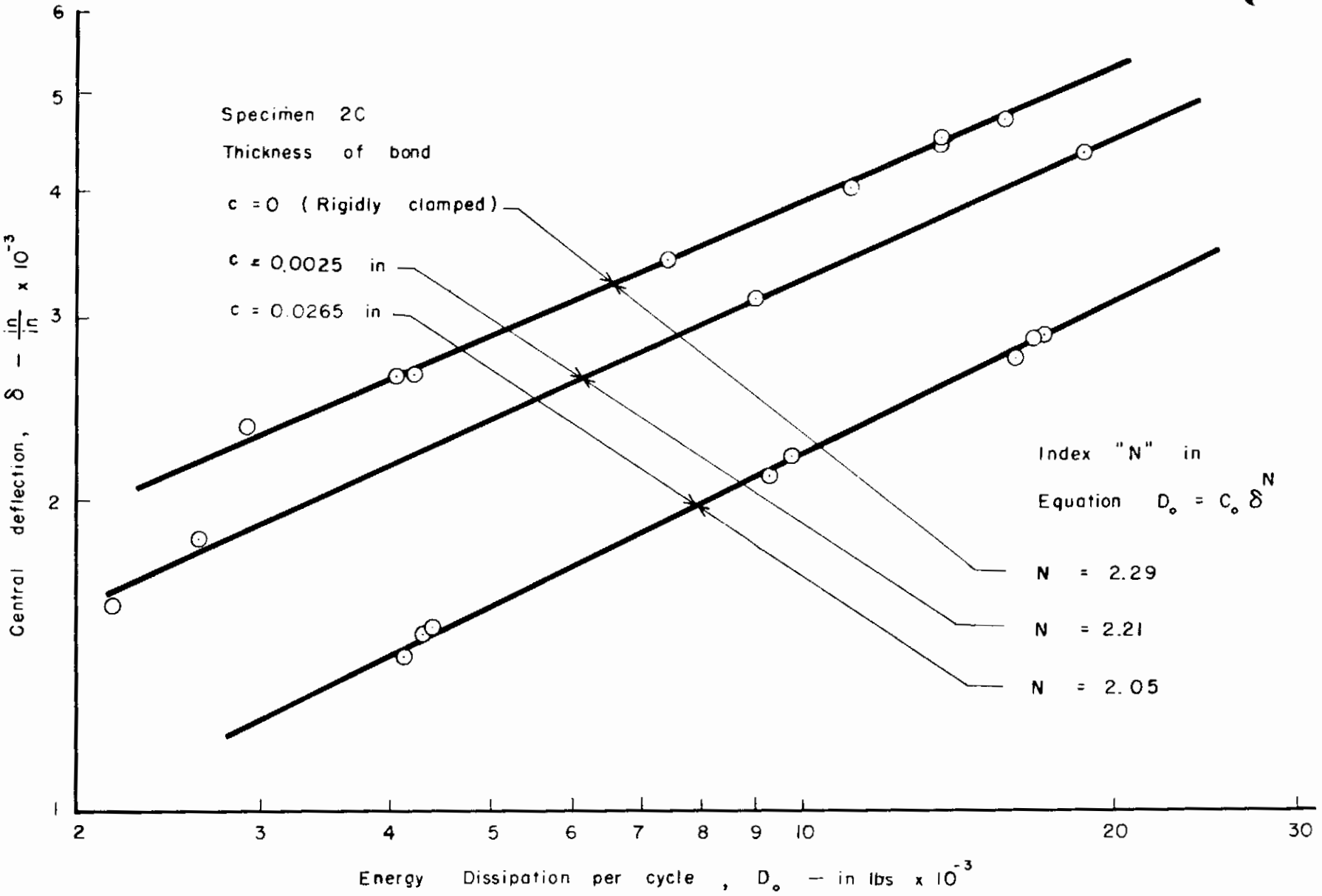

Fig. 14 Energy Dissipation for Model Beam.

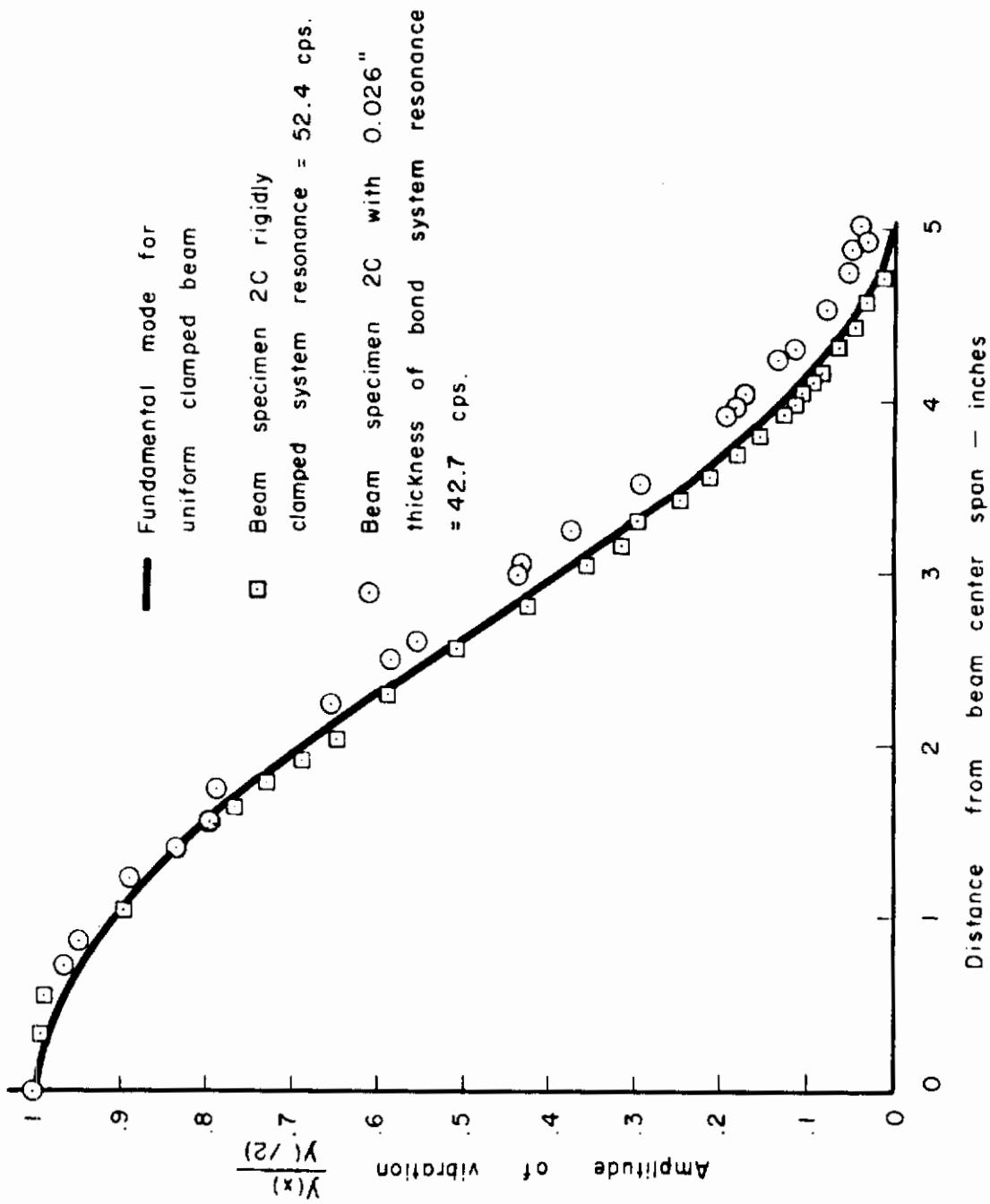

Fig. 15 Mode Shapes.

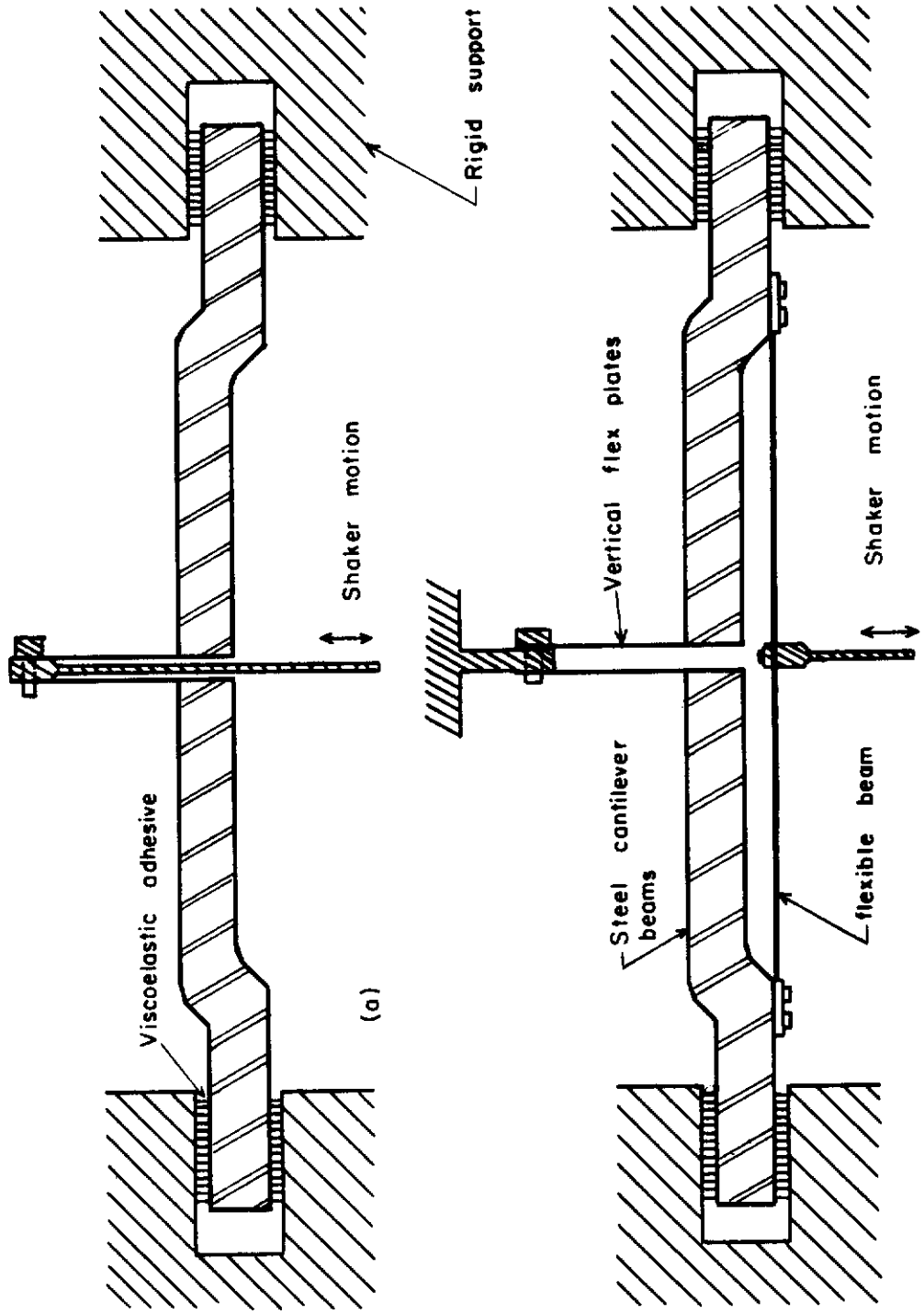

Fig. 16 Articulated Beam.

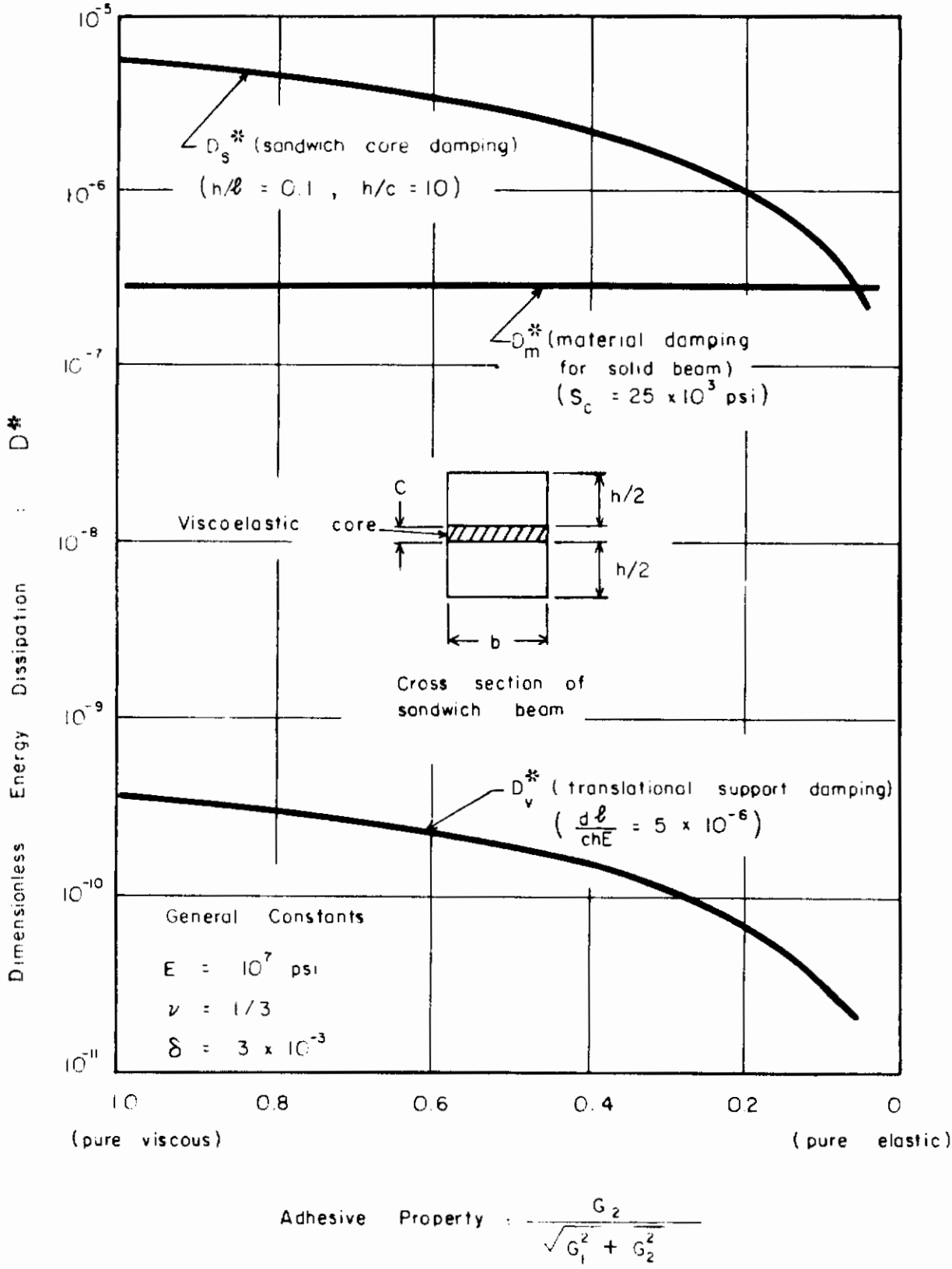

Fig. 18 Comparison of Energy Dissipations for Sandwich Beams.

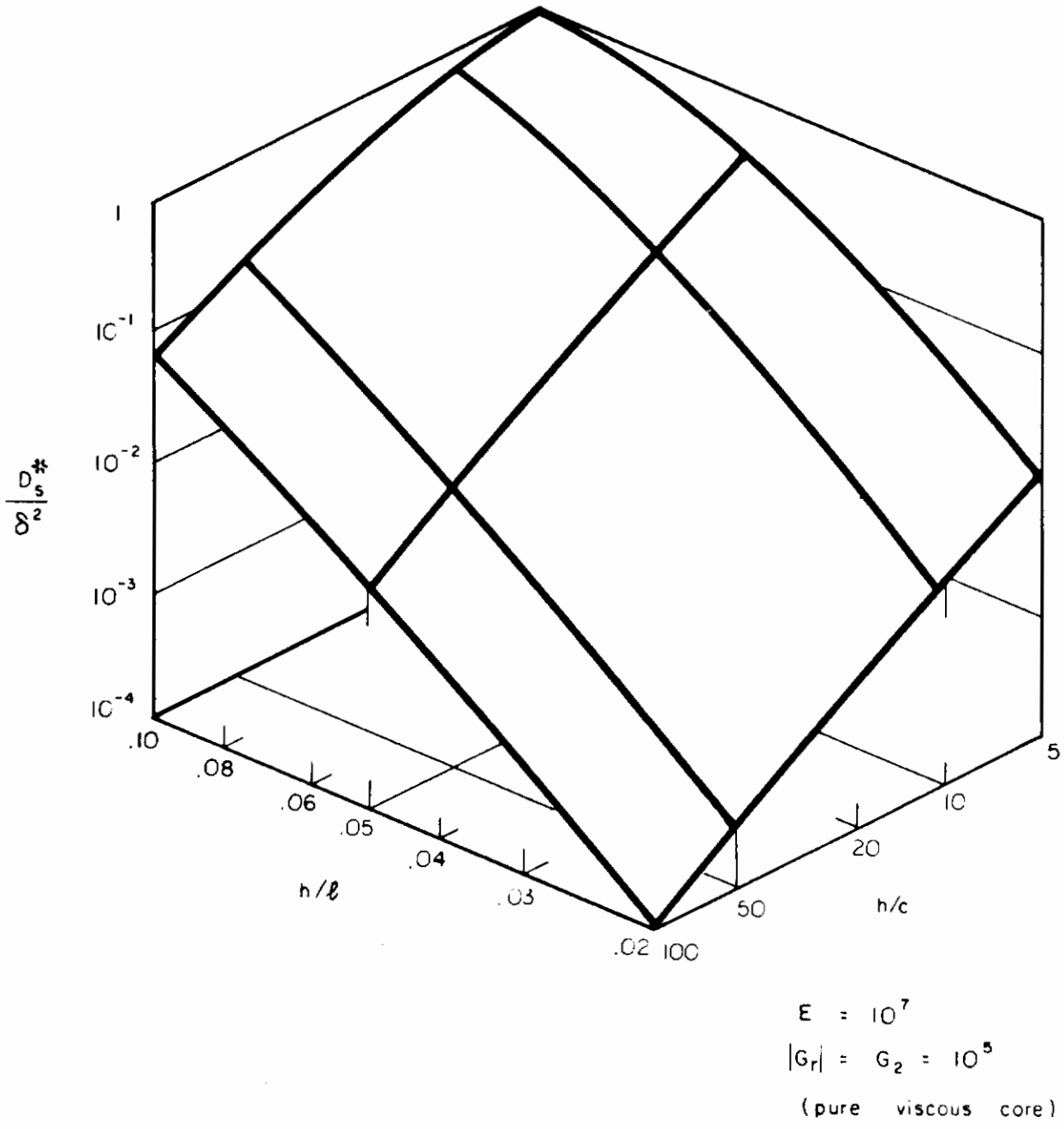

Fig. 19 Optimization of Sandwich Beam Geometry.

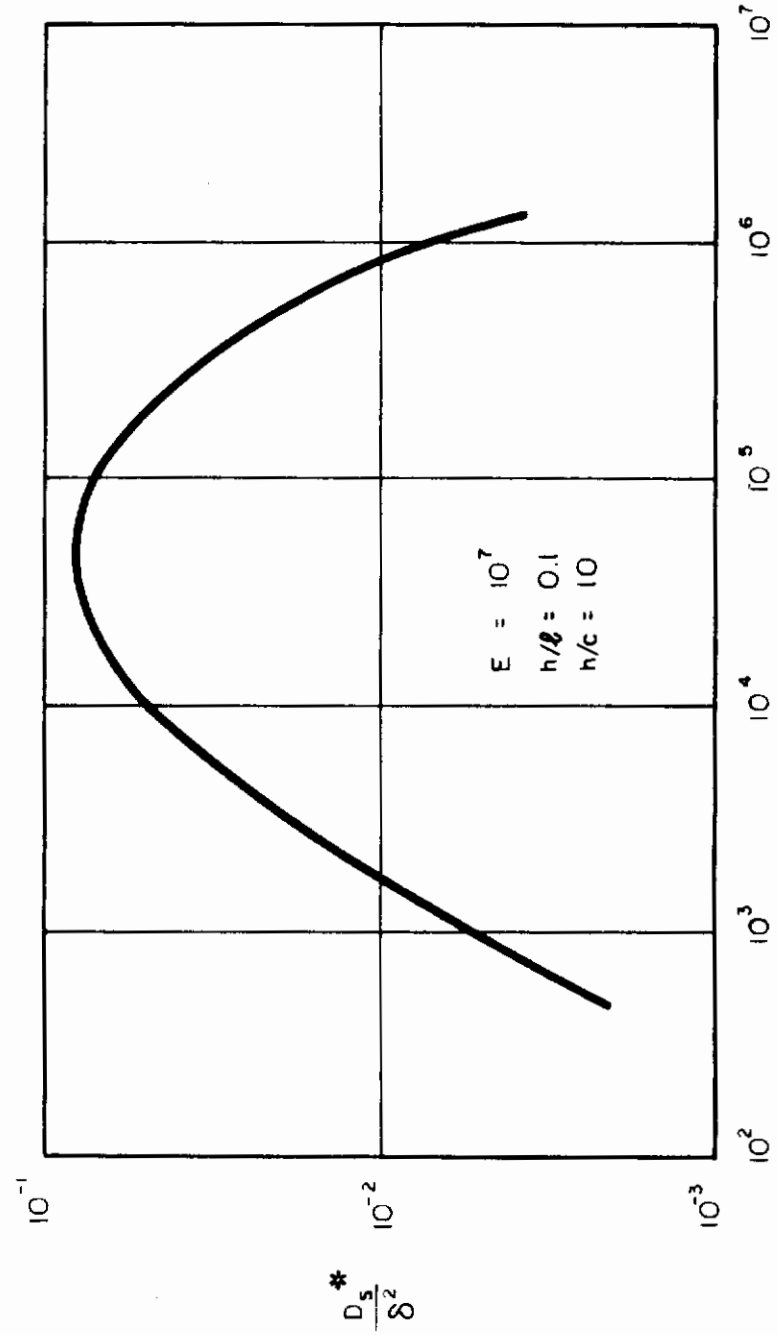

Fig. 20 Optimization of Sandwich Beam Core Properties.